Short communication

# Elucidating the higher stability of vanadium(V) cations in mixed acid based redox flow battery electrolytes

CrossMark

M. Vijayakumar*, Wei Wang*, Zimin Nie, Vincent Sprenkle, JianZhi Hu

*Pacific Northwest National Laboratory, Richland, WA 99352, USA*

HIGHLIGHTS

- Mechanism of $V^{5+}$ higher chemical stability in mixed acid solution is revealed.
- Explains $V^{5+}$ specitation related to its stability using NMR and DFT method.
- Chlorine bonding with di-nuclear $V^{5+}$ cation leads to higher stability.

ARTICLE INFO

ABSTRACT

The vanadium(V) cation structures in mixed acid based electrolyte solution were analyzed by density functional theory (DFT) based computational modeling and $^{51}$V and $^{35}$Cl nuclear magnetic resonance (NMR) spectroscopy. The vanadium(V) cation exists as di-nuclear $[V_2O_3Cl_2 \cdot 6H_2O]^{2+}$ compound at higher vanadium concentrations ($\geq$1.75 M). In particular, at high temperatures ($>$295 K) this di-nuclear compound undergoes ligand exchange process with nearby solvent chlorine molecule and forms chlorine bonded $[V_2O_3Cl \cdot 6H_2O]^{2+}$ compound. This chlorine bonded $[V_2O_3Cl_2 \cdot 6H_2O]^{2+}$ compound might be resistant to the de-protonation reaction which is the initial step in the precipitation reaction in vanadium based electrolyte solutions. The combined theoretical and experimental approach reveals that formation of chlorine bonded $[V_2O_3Cl_2 \cdot 6H_2O]^{2+}$ compound might be central to the observed higher thermal stability of mixed acid based vanadium(V) electrolyte solutions.

© 2013 Elsevier B.V. All rights reserved.

## 1. Introduction

Developing reliable energy storage devices is pivotal to meet the world's growing energy demands. In particular, large scale energy storage devices ($>$kW h) is crucial in constructing efficient and uninterrupted electrical supply grids [1,2]. In recent years, redox flow batteries (RFB) attracted major attention due to its compatibility with intermittent energy conversion devices such as solar and wind energy [3–6]. The redox reaction between redox active species such as vanadium–bromide, iron–chromium, zinc–bromine, and all-vanadium is the basis of RFB operation [5,6]. In particular, all-vanadium based redox flow batteries (VRFB) have been widely recognized as prominent candidate for large-scale storage due to long lifespan, quick response time, deep-discharge capability and low maintenance cost [7–9]. Despite these advantages, VRFB development is plagued by the poor solubility and temperature

stability of vanadium species in acidic electrolyte solutions which ultimately limits the total energy density of the battery [4,6,10–12]. In particular, the vanadium(V) (*i.e.*, $V^{5+}$) species register poor stability at elevated temperatures ($>$310 K) and also at high vanadium concentrations ($>$2 M) under electrolyte solution with conventional sulfuric acid as solvent. This thermal and chemical instability is observed as $V_2O_5$ powder precipitation during the battery operation, which leads to energy loss and failure of the battery. The chemistry behind this poor stability of $V^{5+}$ cations in the pure sulfuric acid based electrolyte solution is recently reported [13]. Similarly, the molecular structure and dynamics of vanadyl cation ($V^{4+}$) in pure sulfuric acid is also reported [14]. Understanding these vanadium solution chemistry has helped us in designing a novel mixed acid based electrolyte system which shows higher thermal and chemical stability, where the solvent is a mixture of sulfuric and hydrochloric acids [15]. This mixed acid based electrolyte system yields nearly double the energy density of conventional sulfuric acid system for the VRFB system due to the higher vanadium(V) stability. To understand the chemistry behind higher thermal and chemical stability of $V^{5+}$ in mixed acid based system,

* Corresponding authors. Tel.: +1 509 372 4097.
  *E-mail addresses:* Vijay@pnnl.gov (M. Vijayakumar), wei.wang@pnnl.gov (W. Wang).

in this work a combined density functional theory (DFT) and nuclear magnetic resonance (NMR) spectroscopic studies were carried out. This interplay between computation and experimental analysis results helped us to derive the chemistry behind higher stability of $V^{5+}$ cations which is discussed herein.

## 2. Experimental

The mixed acid based electrolyte solution contains 1:2 ratio of vanadium to chloride and 1:1 ratio of vanadium to sulfate ions. The 2.5 M vanadium(V) electrolyte solution was prepared using full redox battery cycling method reported previously [15] and diluted with water to explore low concentration effects. The $^{35}Cl$ and $^{51}V$ NMR measurements were performed using a Varian 500 Inova spectrometer ($B_0 = 11.1$ T and $^{35}Cl$ and $^{51}V$ Larmor frequencies are 38.4 and 130.7 MHz respectively). The variable temperature measurements were carried out for every 10 K both during heating and cooling cycles to monitor thermally induced structural changes. The quantitative $^{35}Cl$ and $^{51}V$ NMR spectra were recorded with single pulse measurements at all temperatures using 5 mm NMR tubes with a Varian liquid probe. The $^{35}Cl$ and $^{51}V$ chemical shifts were externally referenced to 5 M aqueous HCl solutions and neat $VOCl_3$ solution respectively ($\delta_{iso} = 0$ ppm). Accurate chemical shifts and line width at each temperature were obtained from fitting the line shapes of the resonance lines using mixed Gaussian and Lorentzian shapes. Quantum chemistry calculations were carried out using the *Amsterdam Density Functional* (ADF-2010) program [16,17]. All DFT calculations were carried out with three different functionals, namely Generalized Gradient Approximation (GGA) based Perdew, Burke, and Ernzerhof (PBE) function [18], Meta-GGA based MO6-L function [19] and hybrid-GGA based Becke, three-parameter, Lee–Yang–Parr (B3LYP) function [20]. The QZ4P (quadruple *Z*, 4 polarization functions, all electron) basis set with Slater type functional implemented in the ADF program is used for both geometry optimization and property calculation [21]. The property calculations such as NMR chemical shift and Hirshfeld charges are carried out from fully optimized molecular structures which were verified with frequency calculation to ensure the proper energy minima. The reaction energy ($\Delta G$) reported here is bonding energy difference between reactants and products.

## 3. Results and discussion

The $V^{5+}$ cations typically exists as the dioxo-aqua-cation $[VO_2(H_2O)_3]^+$ in acidic solutions. The existence of this hydrated $V^{5+}$ cation structure depends on the vanadium concentration and pH values of the solution. For example, Madic et al., reported that high acidity and high vanadium concentrations can lead to the formation of a di-nuclear $[V_2O_3 \cdot 8H_2O]^{4+}$ cation (also denoted as $V_2O_3^{4+}$) [22]. The formation of this di-nuclear structure with increase in vanadium concentration is witnessed as visible color change from yellow to red in mixed acid solutions. The red color indicates the presence of di-nuclear $[V_2O_3 \cdot 8H_2O]^{4+}$ compound **A** in higher vanadium concentrations ($\geq 1.75$ M). Since the VRFB typically operates at higher vanadium concentrations, our discussions will mainly focus on this di-nuclear structure of $V^{5+}$ cations. In particular, under mixed acid solution the chlorine can bond with this di-nuclear compound **A** through a ligand exchange process [23]. Such a ligand exchange process could lead to formation of chlorine bonded di-nuclear $[V_2O_3Cl_2 \cdot 6H_2O]^{2+}$ compound **B** as expressed below,

$$[V_2O_3 \cdot 8H_2O]^{4+} + 2HCl \rightarrow [V_2O_3Cl_2 \cdot 6H_2O]^{2+} + 2H_3O^+ \qquad (1)$$
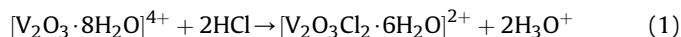
To test the possibility of such a chlorine bonded di-nuclear $[V_2O_3Cl_2 \cdot 6H_2O]^{2+}$ compound **B** we first carried out the DFT based studies. Fig. 1 shows the DFT optimized structure of both di-nuclear $[V_2O_3 \cdot 8H_2O]^{4+}$ compound **A** and chlorine bonded di-nuclear $[V_2O_3Cl_2 \cdot 6H_2O]^{2+}$ compound **B**. Comparing the bonding energy of the reactant and resultant molecules from DFT optimized structure, it is deduced that the chlorine bonding reaction (see Eq. (1)) is energetically favorable ($\sim 9.5$ eV) in mixed acid electrolyte solution. However, it should be noted that the present DFT calculations were carried out using single $V^{5+}$ molecule under gas phase condition. In reality, mixed acid electrolyte system contains concentrated sulfuric and hydrochloric acids exhibiting highly acidic (pH < 0) behavior and contains high concentration of vanadium (>1.5 M). Hence, the DFT calculated reaction energy may not completely represent the mixed electrolyte system. Nevertheless, the exothermic nature observed in DFT calculation suggests the possibility of chlorine complexation with $V^{5+}$ cations in electrolyte solution. To verify the possibility of these anion complexed structures in the redox battery electrolytes, we carried out $^{51}V$ and $^{35}Cl$ NMR measurements on various concentration of $V^{5+}$ under mixed acid based electrolyte solutions.

Fig. 2 shows the $^{51}V$ and $^{35}Cl$ NMR parameters *i.e.*, chemical shift and line width of $V^{5+}$ solutions with different vanadium concentrations of mixed acid system. The NMR peak parameters of high vanadium concentration ($\geq 1.75$ M) are significantly different from their low concentration counterparts. This coincides with the dramatic color change observed in mixed acid based $V^{5+}$ solutions and indicates the di-nuclear compound formations. However, to clearly ascertain the formation of chlorine bonded di-nuclear compound **B** we compared the experimental $^{51}V$ and $^{35}Cl$ NMR chemical shifts with DFT derived di-nuclear compounds **A** and **B** (see Fig. 1). It should be noted that the theoretically calculated chemical shifts depends on choice of DFT functional and basis sets, on the other hand experimental NMR chemical shifts represent the averaged state of molecules due to thermally induced dynamics such as ligand exchange with solvent molecules [24]. Hence, while comparing the theoretical and experimentally observed chemical shift, more attention should be paid to the trends in the chemical shift between the compounds rather than to their actual values. For example, $^{35}Cl$ peaks shows significant shift toward higher frequency (*i.e.* low field shift) at higher vanadium concentration ($\geq 1.75$ M) which agrees with DFT calculated chemical shifts of compound **B** relative to aqueous chlorine from solvent molecules (used as standard $^{35}Cl$ NMR reference in this work). However, $^{51}V$ peaks registers only a small shift (*i.e.*, less than 10 ppm) for entire vanadium concentration under study. This is mostly due to the fact that both mononuclear dioxo-aqua-cation $[VO_2(H_2O)_3]^+$ and di-nuclear compound **A** have similar $^{51}V$ chemical shift as reported in our recent result [25]. Unlike the chemical shift, the peak width of $^{51}V$ NMR shows exponential increase at higher concentrations where the $^{51}V$ line width is large ($\sim 10$ kHz) and covers DFT calculated chemical shift ranges of both compounds **A** and **B**. Combining these results, it is clear that at higher concentrations, di-nuclear compounds are the dominant species in the solution. This concentration dependent $^{51}V$ and $^{35}Cl$ NMR analysis also suggests that it is possible to have both di-nuclear compounds **A** and **B** in the high concentration mixed acid solutions. Since, compound **B** forms due to the ligand exchange between vanadium bound water molecule and chlorine from solvent molecule (see Eq. (1)), the concentration of compound **B** would greatly depend on the vanadium concentration and temperature of the solution. The higher vanadium concentration means smaller solvent to counter anion ratio which can lead to highly chlorine populated vanadium solvation sphere and subsequently facilitate formation of chlorine bonded di-nuclear compound **B** in the electrolyte solution. Similarly, the thermal energy can also assist the ligand exchange process to form compound **B**. This means the ratio of concentration between di-nuclear
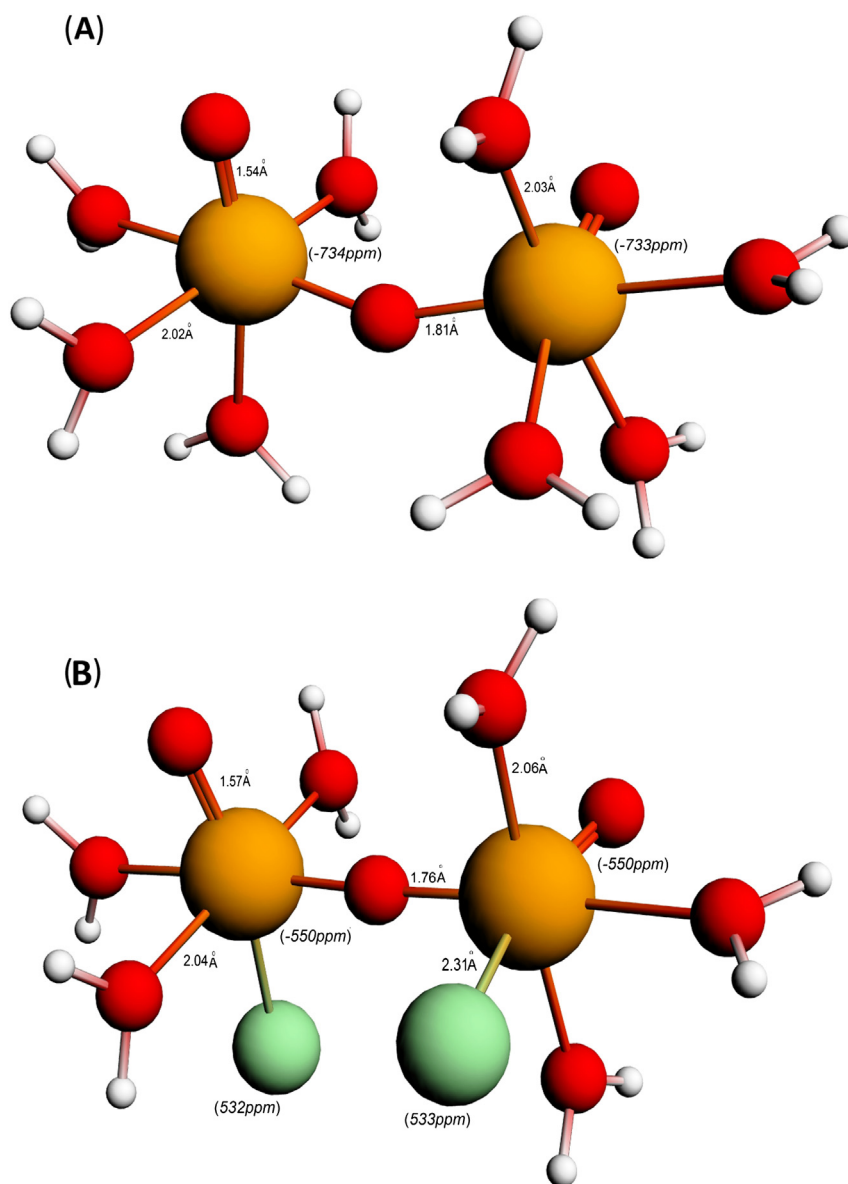
**Fig. 1.** Geometry-optimized structures for pristine di-nuclear $[V_2O_3 \cdot 8H_2O]^{4+}$ compound (**A**) and chlorine bonded $[V_2O_3Cl_2 \cdot 6H_2O]^{2+}$ compound **B** using DFT theory with B3LYP functional and QZ4P basis electron set (see text for details). The vanadium, oxygen, chlorine and proton atoms are represented as yellow, red, green and white spheres respectively. The calculated chemical shifts (noted in parenthesis) are in ppm and bond lengths are noted in Angstrom (For interpretation of the references to color in this figure legend, the reader is referred to the web version of this article.).

compounds **A** and **B** would be mainly determined by the vanadium concentration and temperature of the solution.

To understand the effect of temperature on this ligand exchange process and chemical stability of di-nuclear compounds **A** and **B**, we carried out variable temperature $^{51}$V and $^{35}$Cl NMR measurements. Fig. 3 shows the variable temperature $^{51}$V and $^{35}$Cl NMR measurements of 2.0 M vanadium(V) cations in mixed acid electrolyte solution. All the variable temperature measurements were done during both cooling and heating cycles and NMR peak trends are highly reversible indicating higher thermal stability of $V^{5+}$ cations under mixed acid based system. At high temperatures ($\geq$295 K) the $^{35}$Cl NMR shows emergence of new peak at relatively higher frequency ($\sim$360 ppm) than the solvent chlorine peak ($\sim$50 ppm). The appearance of a new peak at higher frequency agrees with DFT calculated chlorine chemical shift of compound **B** (see Fig. 2). Similarly, $^{51}$V NMR also shows formation of new peak at higher frequency ($\sim$ −220 ppm) in accordance with DFT calculated vanadium

chemical shift of compound **B**. The formation of new peaks under both $^{51}$V and $^{35}$Cl NMR measurements clearly support our hypothesis about the formation of chlorine bonded compound **B** in high vanadium concentration mixed acid system. Interestingly, the intensity of this new peak increases with increase in temperature indicating that formation of compound **B** is mainly through thermally activated ligand exchange process as shown in Eq. (1). This means, at low temperatures (<295 K) the mixed electrolyte system is dominated by di-nuclear $[V_2O_3 \cdot 8H_2O]^{4+}$ compound **A** whereas at higher temperatures chlorine bonded di-nuclear $[V_2O_3Cl_2 \cdot 6H_2O]^{2+}$ compound **B** will also be the part of solution. Now the observed higher thermal stability of the $V^{5+}$ cations under mixed electrolyte system can be due to the formation of chlorine bonded compound **B** at higher temperatures. To validate this claim we need to analyze the chemical stability of both compounds **A** and **B**.

The poor thermal stability of $V^{5+}$ cations under traditional sulfuric acid based electrolyte system is due to de-protonation with
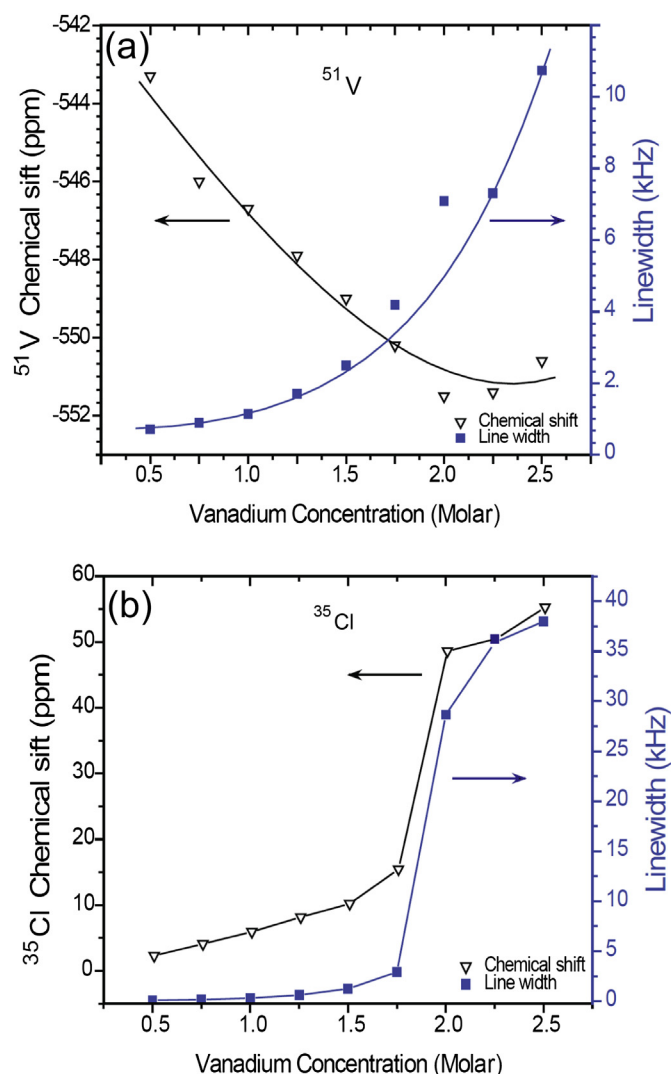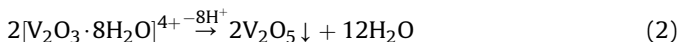
**Fig. 2.** The vanadium concentration dependent (a) $^{51}V$ and (b) $^{35}Cl$ NMR resonance peak parameters for mixed acid based electrolyte solutions measured at a magnetic field of 11.7 T. The lines are to guide the eye and don't represent any mathematical analysis.



**Fig. 3.** Variable temperature (a) $^{51}V$ and (b) $^{35}Cl$ NMR analysis for 2.0 M vanadium (V) mixed acid based solutions measured at a magnetic field of 11.7 T. The color lines represent the deconvolution analysis using Gaussian/Lorentizan type peaks (For interpretation of the references to color in this figure legend, the reader is referred to the web version of this article.).

subsequent hydrolysis reaction that led to the $V_2O_5$ precipitations [13]. This de-protonation initiated precipitation reaction under dinuclear compound **A** can be described as,

$$2[V_2O_3 \cdot 8H_2O]^{4+} \overset{-8H^+}{\rightarrow} 2V_2O_5 \downarrow + 12H_2O \qquad (2)$$

Unlike the traditional sulfuric acid based system, the mixed acid based electrolytes don't register any such precipitation reaction even at higher temperatures ($\sim 320$ K) which could be due to the presence of compound **B** in the electrolyte system. Typically, the possibility of de-protonation is the major factor in determining the vanadium chemical stability in the electrolyte solution [13,26]. This chlorine bonded di-nuclear $[V_2O_3Cl_2 \cdot 6H_2O]^{2+}$ compound **B** may offer relatively higher resistant to the de-protonation reactions (see Eq. (2)) and thereby register higher thermal stability. Now, the possibility of de-protonation in the pristine compound **A** and chlorine bonded di-nuclear compound **B**, can be explored by analyzing the Hirshfeld partial charges through DFT calculation. The Hirshfeld partial charges can provide clear picture about electron density at the oxygen atom of water molecules bonded with vanadium molecules [26,27]. Fig. 4 shows averaged Hirshfeld
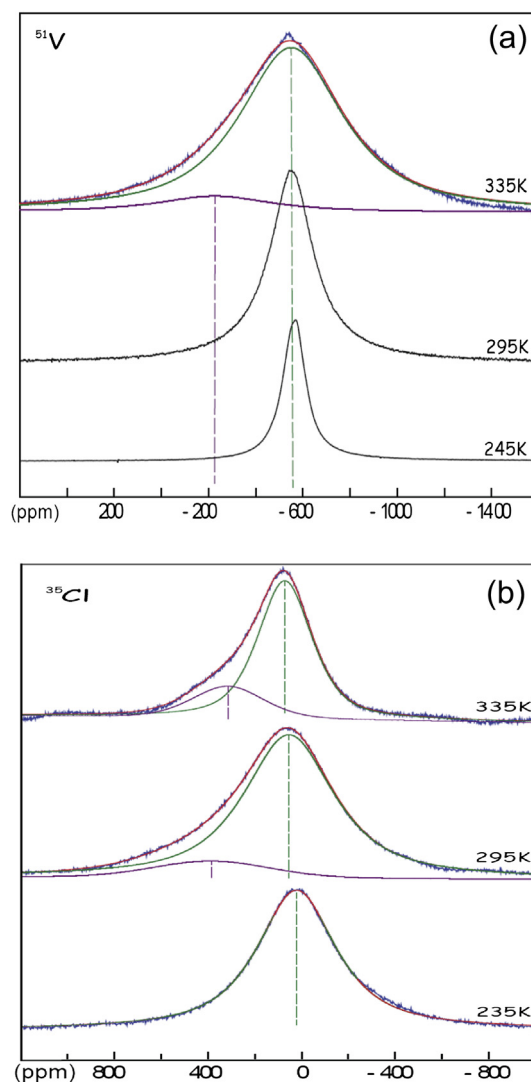
charges for all the oxygen in optimized structure of the pristine and chlorine bonded di-nuclear molecules and compared with diaquo-hydrogen ion $[H_5O_2]^+$. It is well known that this diaquo-hydrogen ion has greater ability to donate proton (i.e. de-protonation reaction) which is reflected by the lower partial charge of its oxygen atoms. In comparison, the average charge of the oxygen atoms at vanadium(V) molecules (both compounds **A** and **B**) is higher which shows it is hard to remove proton from these molecules [26]. It is interesting to note that average charge of oxygen for chlorine bonded compound **B** is even higher than the pristine compound **A** which suggests that the de-protonation is relatively harder for these chlorine complexed species. This might be due to the electron donor ability of chlorine molecule which can increase the electron density at vanadium and thereby reduce its interaction with oxygen at the solvating water molecules. This is also witnessed as increase in vanadium—oxygen bond length for anion complexed species (see Fig. 1). In this scenario, the oxygen molecule will mostly share electron with hydrogen atoms and forms relatively rigid water molecule which can resist the de-protonation reactions. Overall, bonding of chlorine with $V^{5+}$ cation would reduce its de-
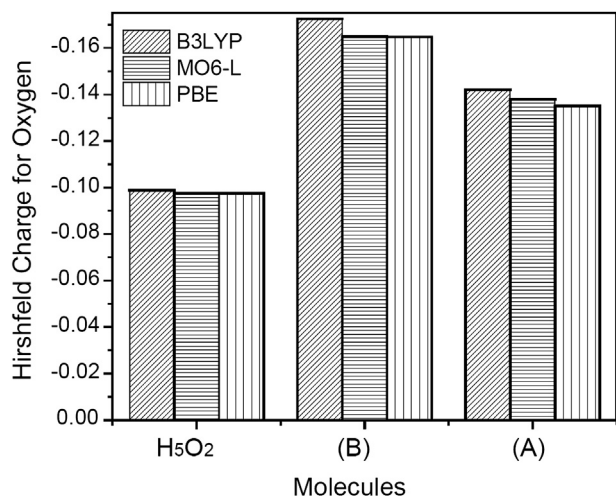
**Fig. 4.** Average *Hirshfeld* charge for oxygens in pristine di-nuclear $[V_2O_3 \cdot 8H_2O]^{4+}$ compound (**A**) and chlorine bonded $[V_2O_3Cl_2 \cdot 6H_2O]^{2+}$ compound **B** calculated using hybrid B3LYP function with QZ4P basis set (see text for details). The diaquo-hydrogen $[H_5O_2]^+$ is also shown for comparing the Hirshfeld charge with proton donor ability (see Ref. [25] for more details).

protonation ability and thereby restrict the thermally induced precipitation reaction in electrolyte solution. On the other hand, the absence of chlorine molecules in pure sulfuric acid based electrolytes causes pristine di-nuclear compound **A** to undergo deprotonation and subsequent precipitation reaction at high temperatures (>310 K) as shown in Eq. (2).

## 4. Conclusions

The vanadium(V) cation structure in mixed acid based electrolyte solution is studied using DFT based computational method and NMR spectroscopy methods. The DFT studies suggests that chlorine bonded di-nuclear $[V_2O_3Cl_2 \cdot 6H_2O]^{2+}$ compound **B** is energetically favorable than the pristine di-nuclear $[V_2O_3 \cdot 8H_2O]^{4+}$ compound **A**. The NMR spectroscopy confirms the presence of chlorine bonded di-nuclear cation in higher vanadium concentration ($\leq 1.75$ M) solutions. The increase in temperature facilitates the formation of chlorine bonded di-nuclear compound **B** through ligand exchange process. Apparently the chlorine bonded $[V_2O_3Cl_2 \cdot 6H_2O]^{2+}$ compound **B** shows more resistant to the de-protonation reaction which is the initial process in the $V_2O_5$ precipitation reaction. Therefore, the higher thermal stability of $V^{5+}$ cations in mixed acid system arise due to the formation of chlorine bonded vanadium species which can resist the de-protonation and subsequent precipitation reactions.

## Acknowledgments

## References

[1] Z. Yang, J. Zhang, M.C.W. Kintner-Meyer, X. Lu, D. Choi, J.P. Lemmon, J. Liu, Chemical Reviews 111 (2011) 3577–3613.
[2] B. Dunn, H. Kamath, J.-M. Tarascon, Science 334 (2011) 928–935.
[3] W. Wang, Q. Luo, B. Li, X. Wei, L. Li, Z. Yang, Advanced Functional Materials 23 (8) (2013) 970–986, http://dx.doi.org/10.1002/adfm.201200694.
[4] P. Leung, X. Li, C. Ponce de Leon, L. Berlouis, C.T.J. Low, F.C. Walsh, RSC Advances 2 (2012) 10125–10156.
[5] A. Weber, M. Mench, J. Meyers, P. Ross, J. Gostick, Q. Liu, Journal of Applied Electrochemistry 41 (2011) 1137–1164.
[6] M. Skyllas-Kazacos, M.H. Chakrabarti, S.A. Hajimolana, F.S. Mjalli, M. Saleem, Journal of the Electrochemical Society 158 (2011) R55–R79.
[7] C. Fabjan, J. Garche, B. Harrer, L. Jörissen, C. Kolbeck, F. Philippi, G. Tomazic, F. Wagner, Electrochimica Acta 47 (2001) 825–831.
[8] M. Skyllas-Kazacos, F. Grossmith, Journal of the Electrochemical Society 134 (1987) 2950–2953.
[9] M. Skyllas-Kazacos, M. Rychcik, R.G. Robins, A.G. Fane, M.A. Green, Journal of the Electrochemical Society 133 (1986) 1057–1058.
[10] N. Kausar, R. Howe, M. Skyllas-Kazacos, Journal of Applied Electrochemistry 31 (2001) 1327–1332.
[11] M. Kazacos, M. Cheng, M. Skyllas-Kazacos, Journal of Applied Electrochemistry 20 (1990) 463–467.
[12] M. Skyllas-Kazacos, C. Menictas, M. Kazacos, Journal of the Electrochemical Society 143 (1996) L86–L88.
[13] M. Vijayakumar, L. Li, G. Graff, J. Liu, H. Zhang, Z. Yang, J.Z. Hu, Journal of Power Sources 196 (2011) 3669–3672.
[14] M. Vijayakumar, S.D. Burton, C. Huang, L. Li, Z. Yang, G.L. Graff, J. Liu, J. Hu, M. Skyllas-Kazacos, Journal of Power Sources 195 (2010) 7709–7717.
[15] B.B. Hurisso, K.R.J. Lovelock, P. Licence, Physical Chemistry Chemical Physics 13 (2011) 17737–17748.
[16] G. Schreckenbach, T. Ziegler, Journal of Physical Chemistry 99 (1995) 606–611.
[17] G. te Velde, F.M. Bickelhaupt, E.J. Baerends, C.F. Guerra, S.J.A.v. Gisbergen, J.G. Snijders, T. Ziegler, Journal of Computational Chemistry 22 (2001) 931–967.
[18] J.P. Perdew, K. Burke, M. Ernzerhof, Physical Review Letters 77 (1996) 3865–3868.
[19] Y. Zhao, D. Truhlar, Theoretical Chemistry Accounts: Theory, Computation, and Modeling (Theoretica Chimica Acta) 120 (2008) 215–241.
[20] A.D. Becke, The Journal of Chemical Physics 98 (1993) 5648–5652.
[21] M. Krykunov, T. Ziegler, E.v. Lenthe, International Journal of Quantum Chemistry 109 (2009) 1676–1683.
[22] C. Madic, G.M. Begun, R.L. Hahn, J.P. Launay, W.E. Thiessen, Inorganic Chemistry 23 (1984) 469–476.
[23] L. Li, S. Kim, W. Wang, M. Vijayakumar, Z. Nie, B. Chen, J. Zhang, G. Xia, J. Hu, G. Graff, J. Liu, Z. Yang, Advanced Energy Materials 1 (2011) 394–400.
[24] R. Bjornsson, H. Fruchtl, M. Buhl, Physical Chemistry Chemical Physics 13 (2011) 619–627.
[25] S. Kim, M. Vijayakumar, W. Wang, J. Zhang, B. Chen, Z. Nie, F. Chen, J. Hu, L. Li, Z. Yang, Physical Chemistry Chemical Physics 13 (2011) 18186–18193.
[26] M. Vijayakumar, L. Li, Z. Nie, Z. Yang, J. Hu, Physical Chemistry Chemical Physics 14 (2012) 10233–10242.
[27] F.L. Hirshfeld, Theoretical Chemistry Accounts: Theory, Computation, and Modeling (Theoretica Chimica Acta) 44 (1977) 129–138.